A 4096 Element Continuous Facesheet MEMS Deformable Mirror for High-Contrast Imaging

S.A. Cornelissen*[1], P.A. Bierden[1], T.G. Bifano[1,2]

[1]Boston Micromachines Corporation, 30 Spinelli Place, Cambridge, MA 02138,
[2] Boston University Photonics Center, 8 Saint Mary's St., Boston, MA 02215

ABSTRACT

This paper presents the progress in the development of a 4096 element MEMS deformable mirror, fabricated using polysilicon surface micromachining manufacturing processes, with 4μm of stroke, a surface finish of less than 10nm RMS, a fill factor of 99.5%, and bandwidth greater than 5kHz. The packaging and high speed drive electronics for this device, capable of frame rates of 22 kHz, are also presented.

Keywords:
Deformable mirror, MEMS, adaptive optics, wavefront correction

1. INTRODUCTION

A 4096 element continuous facesheet deformable mirror system is being developed for the Gemini Planet Imaging instrument, for high-order wavefront aberrations correction to achieve contrast ratios of 10^7-10^8 required to directly detect Jupiter-like planets outside of our solar system that are a billion times fainter than the sun and obscured by light from their parent star, atmospheric aberrations, and optical imperfections in the imaging system [1]. The deformable mirror (DM) design and fabrication is based on a commercially available, 1024 element MEMS (micro electro mechanical systems) DM that has been demonstrated to be capable of flattening a wavefront 0.54nm RMS within the active control band (12.8nm RMS total), in a high-contrast imaging testbed using a 13-bit, closed-loop control system [2]. To achieve the desired performance for the Gemini Planet Imager this DM design is being extended to 4096 elements with 4μm of mechanical stroke, a surface figure better than 10nm RMS, and a bandwidth of 2.5 kHz. The DM is mounted and wirebonded in a ceramic carrier to provide structural support on electrical interconnections. Eight high density flex cables connect the DM to the drive electronics which provides 4096 channels of parallel, high voltage signals to allow control of each individual DM actuator with 14-bit precision.

2. DEFORMABLE MIRROR ARCHITECTURE

MEMS deformable mirrors produced by Boston Micromachines Corporation (BMC) are based on the surface-micromachined, poly-silicon double cantilever actuator architecture pioneered at Boston University [3,4], illustrated in figure 1. The device structure consists of actuator electrodes underneath a double cantilever flexure, that is electrically isolated from the electrodes and maintained at a ground potential. The actuators are arranged in a 64x64 grid, on a pitch of 400μm, and the flexible mirror surface is connected to the center of each actuator through a small attachment post that translates the actuator motion to a mirror surface deformation.

This MEMS DM architecture allows for local deformation of the mirror membrane with an influence function of 26-32% on its nearest neighbor. Figure 2 shows wavefront measurements generated using a 140 element, 2.5μm stroke, BMC MEMS DM in a closed-loop system, demonstrating the ability of the DM to take the shape of high-order Zernike terms.

MEMS Adaptive Optics II, edited by Scot S. Olivier, Thomas G. Bifano, Joel A. Kubby,
Proc. of SPIE Vol. 6888, 68880V, (2008) · 0277-786X/08/$18 · doi: 10.1117/12.770620

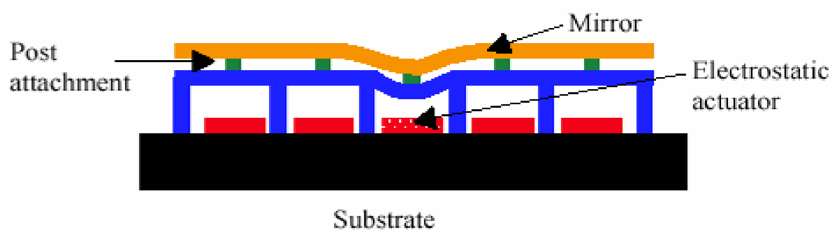

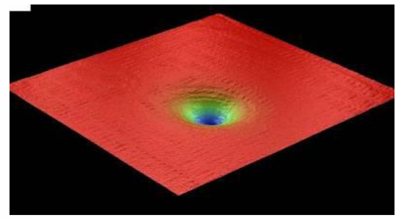

Figure 1. Illustration of cross-section of 1x3 electro-statically actuated MEMS deformable mirror (left); Optical profiler measurement of mirror surface figure of a continuous facesheet BMC DM resulting from actuation of a single element (right). The influence of the single element deflection only affects its immediate neighbors leaving the rest of the mirror surface unchanged.

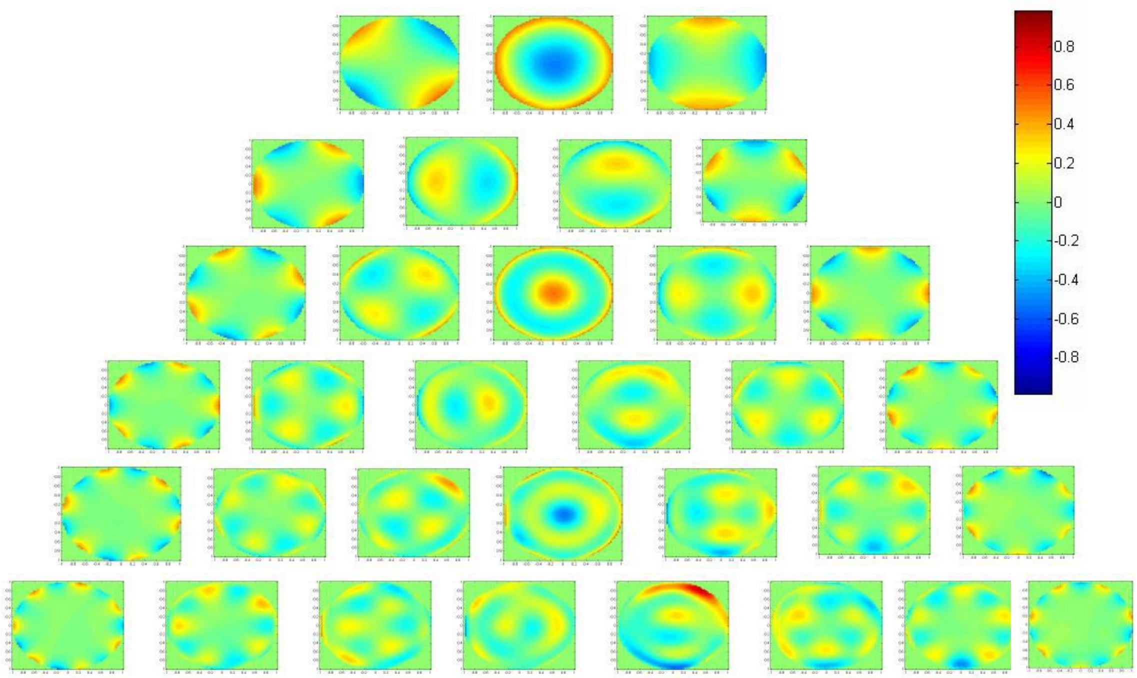

Figure 2. Zernike shapes made by a 2.5μm stroke BMC DM, from 2nd to 7th order (orders by row). Measurements made using a Shack-Hartmann wavefront sensor in a closed-loop control system.

Element deflection is achieved using electrostatic actuators that perform without hysteresis. As illustrated in figure 3, the actuator consists of a double cantilever flexure and the fixed electrode, separated by gap, ***g***. An attractive electrostatic force results when a potential difference is applied across this gap resulting in a downward deflection of the actuator flexure. The electrostatic force is counteracted by the mechanical restoring force of the flexure that provides stable and repeatable actuator control. Using shaped electrodes and perforated double cantilever flexure designs the stable operating range can be extended to over 50% of the surface normal gap to minimize drive voltages and ease manufacturability.

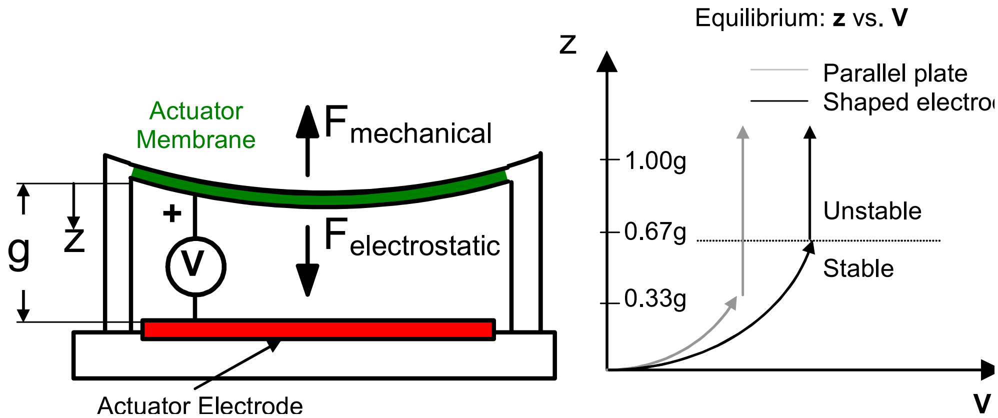

Figure 3. Schematic of electrostatic actuation of a double cantilever flexure used in the MEMS DM design.

3. 4096 ELEMENT MEMS DM DESIGN

A 68x68 element actuator array, supporting a 26.8mm mirror facesheet is located in the center of a 49mm single crystal silicon die, as shown in figure 4. Although the active aperture is 64x64 elements, two rows of elements are used around the periphery of the active area to eliminate edge affects caused by thin film stresses that result in actuator performance variations; adding these dummy elements makes the performance of all the 4096 element uniform. The additional rows also reduce optical edge effects resulting from the CMP processes which induce a rounding of the edge elements that may not be compensated for using the DM actuators. Small holes, 18 per element, are etched in the mirror facesheet and yield a fill factor of ~99.5%. The small holes are required for device manufacturing and to control squeeze film damping that affects the dynamic response of the device. Polysilicon wire traces are routed to four rows of bond pads around the periphery of the die.

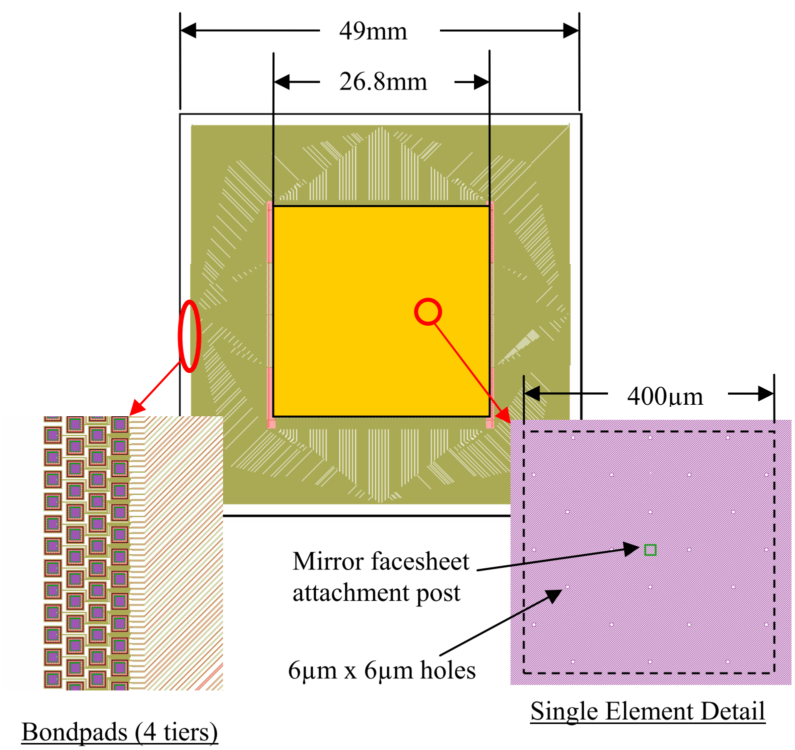

Figure 4. Layout of 4096 element device.

The device performance goals to enable high-contrast imaging in the Gemini Planet Imager instrument are listed in Table 1 below.

Table 1. 4096 Element MEMS Deformable Mirror Requirements

Description	**Requirement**
Pixel count	4096 (64x64 array)
Square Pitch	400 µm
Stroke	3 µm, after mirror is fully flattened to within 70 (RMS)
Fill Factor	99%
Active Aperture size	19.2 mm (48 actuator diameter @ 400µm pitch)
Pixel surface finish (RMS)	<10 nm
Pixel surface finish (P-V)	3 times "Pixel surface finish (RMS)"
Bandwidth	2.5 kHz
Inter-Actuator Stroke	1µm
Yield	100% of actuators on a 48 actuator diameter circular aperture function to spec.
Operating Temperature	-5C

4. MEMS DM FABRICATION PROCESS

The 4096 element DM is fabricated using surface micromachining batch-fabrication techniques. The custom fabrication process, illustrated in figure 5, uses four layers of poly-silicon (poly) alternating with dielectric films and two sacrificial layers of phosphosilicate glass (PSG). For batch processing, 150mm diameter silicon wafers are used as substrates. A low stress silicon nitride layer is deposited, lithographically patterned, and etched to allow electrical access to the substrate. The first layer of poly-silicon is deposited, patterned, and etched to create the wire routing for the array. This is followed by the deposition of a silicon nitride film that electrically isolates the electrical wiring layer. Small vias are etched in the dielectric film to allow interconnections to each wire. A second polysilicon film is deposited, patterned and etched to form the actuator electrodes. To define the surface normal gap between the actuator flexure and electrode, a thick sacrificial silicon dioxide film is deposited over the second electrode layer. The thickness of this film is controlled to within 5% to achieve the desired actuator stroke and to maintain operating voltages below 300V. This film is patterned and etched to provide anchor points for the actuator flexures created by a third structural layer of polysilicon deposited over the sacrificial oxide.

A second, sacrificial silicon dioxide layer is deposited over the actuator flexures, and chemopolished to remove undesired topography resulting from features etched in the underlying layers. The chemopolish process greatly improves the surface finish of the final poly-silicon mirror layer. This film is then patterned and etched to create mirror post attachment points and to serve as a spacer between the actuator and the mirror, providing sufficient clearance for the mirror membrane for its 4µm range of motion. A final poly-silicon layer is deposited, patterned, and etched to create the mirror and its post attachments to the center of the actuator flexure. This final polysilicon film is touch polished using CMP to further improve the optical quality of the mirror surface. Pad metal is patterned and deposited onto the bondpads through a liftoff process to facilitate wire bonding of the device. The sacrificial silicon dioxide films are removed with a hydrofluoric acid etch, releasing the structural poly-silicon.

To achieve high reflectivity, a gold coating is applied to the DM, using electron beam evaporation, after the device has been released. The device is mounted in a ceramic chip carrier to provide structural support and electrical interconnections to the DM actuators. The 4096 electrical interconnections are made using wirebonds between the DM and the chip carrier.

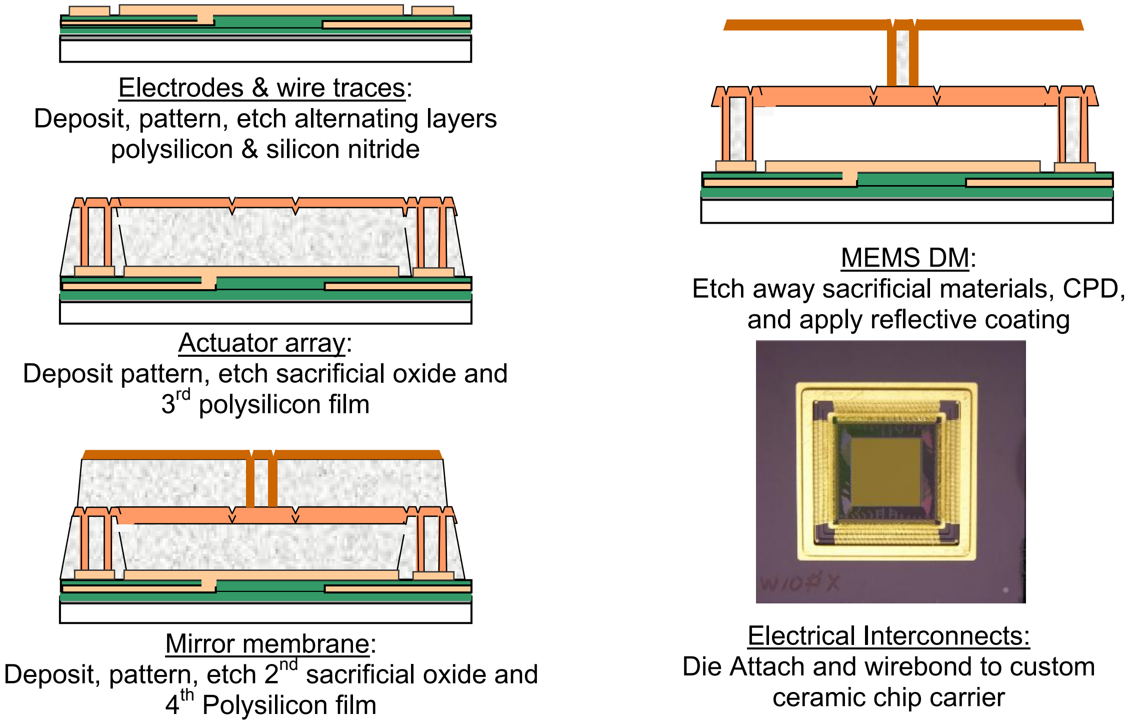

Figure 5. Fabrication process flow used to BMC's MEMS DMs. A cross-section of a single actuator is shown.

5. DM SURFACE FIGURE

The surface figureof the first batch of fabricated devices, measured using a ZYGO NewView 6300 Optical Profiler, is shown in figures 6 and 7. A single element surface finish of less than 6nm RMS and ~40nm P-V has been achieved. Most of the P-V error results from the conformal nature of the deposition processes used during fabrication that cause underlying features to print through on the subsequent layers.

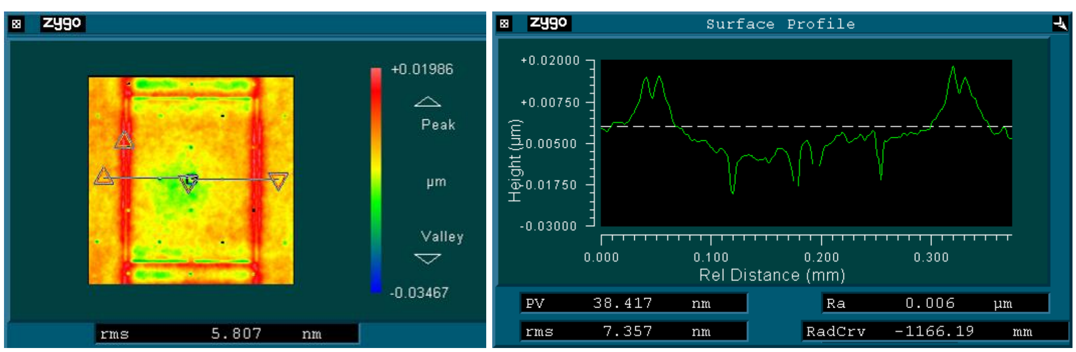

Figure 6. Single element surface measurements of MEMS DM with a surface finish of <6nm RMS and 39nm P-V.

The unpowered surface figure of the full DM aperture, shown in figure 7, has a radius of curvature (ROC) of 17m, resulting in a peak-to-valley bow of ~4µm in a circular aperture of 25.2mm. This radius of curvature is attributed mainly to the overall bow of the silicon substrate induced by a mismatch of film stresses on its front and back side. These stresses result from the fact that all the thin films deposited on the substrate during fabrication are deposited on both front and back side but only those on the front side undergo surface micromachining processes, and the sacrificial materials on the front side are largely removed.

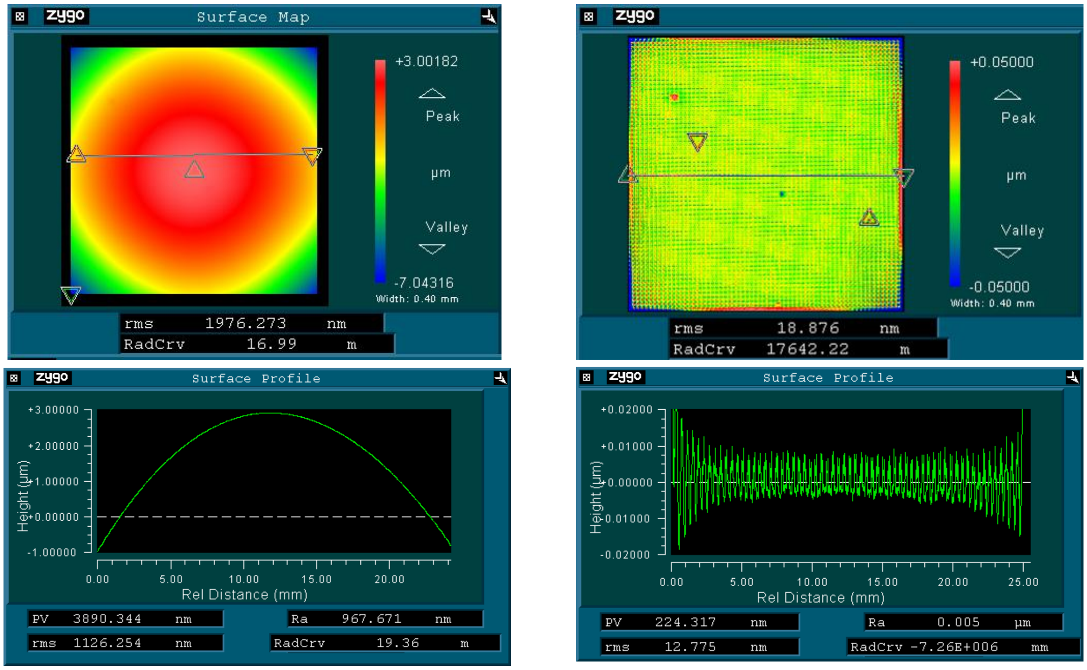

Figure 7. Surface figure measurements of unpowered 4096 element MEMS showing an overall ROC of 17m over a 25.2mm aperture (left). Applying a high pass filter (λ = 1.2mm (corresponding to 3 elements)) to the surface data (right) shows the surface figure error that may be outside of the control band (>2.5/mm).

Removal of some of the backside films can mitigate excessive wafer bow although this process also affects the stresses in the DM actuator flexure and mirror facesheet films which in turn affect the electromechanical performance as well as the optical quality of the device. To investigate non-uniformities in the DM surface figure at spatial frequencies that lie outside of the DM control band – errors within spatial frequencies that are larger than the pitch of the DM elements of 2.5/mm – a high pass filter of 0.83/mm (3 DM elements) is applied to the data. As shown in figure 7, the P-V surface figure error over all but the very edges of the active aperture is within 30nm P-V.

6. DEVICE PACKAGING

A ceramic chip carrier was designed and fabricated to provide electrical interconnections from external drive electronics to each of the 4096 elements of the DM and to provide mechanical support.

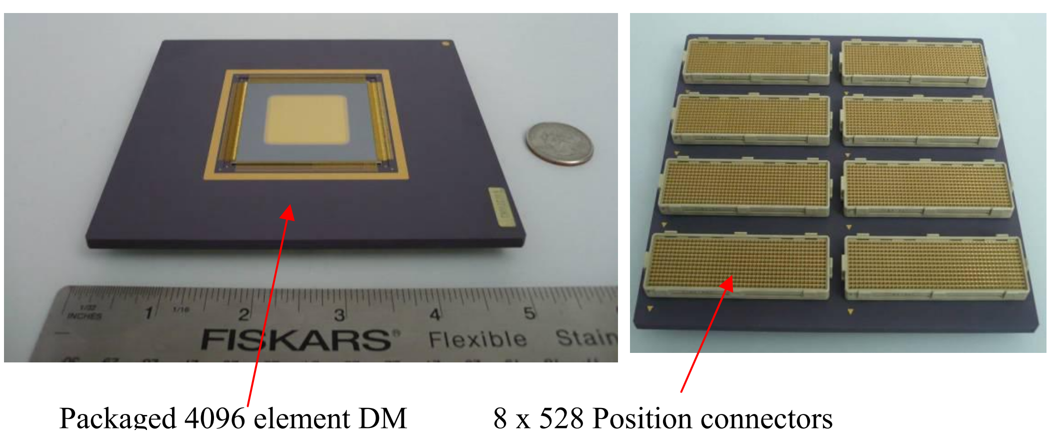

Figure 8. 4096 element MEMS DM mounted and wirebonded in a ceramic carrier that provides electrical interconnection to each element of the DM (Left). Eight 528 pin connectors are assembled to back side of ceramic carrier (Right).

The package, shown in figure 8, was designed with 4 tiers of bond fingers around the edge of the central cavity to allow for wirebonding to the DM bondpads, and Land Grid Array (LGA) pads on the back side to which eight 528 position connectors are attached. High density interface cables attach directly to the connectors on the back side of the package.

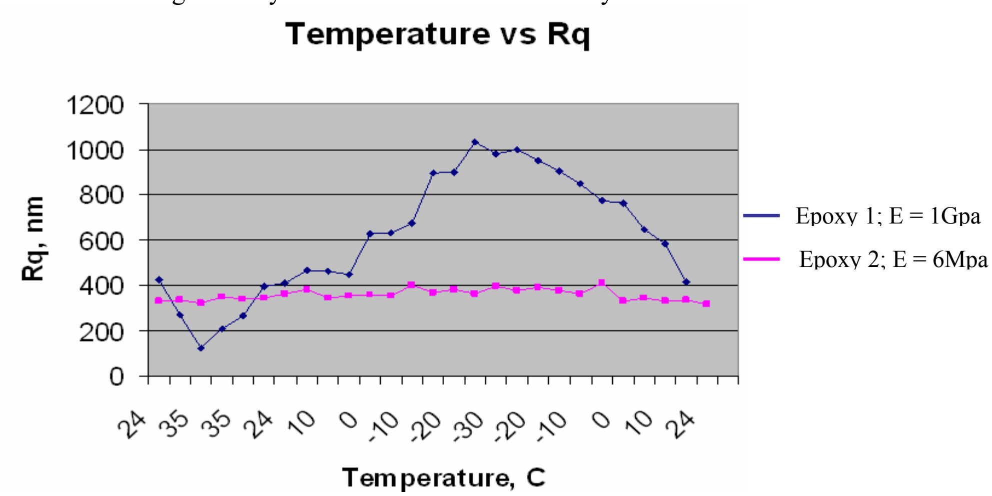

Figure 9. Comparison of the effect of the elastic modulus of the die attach adhesive on surface figure of an unpowered, 140 element MEMS DM packaged in an Alumina chip carrier as a function of temperature. Using an adhesive with a modulus of 6 MPa minimized the change in DM surface figure between -30C and 24C.

To minimize stresses induced on the DM that would affect the device performance when operating at low temperatures, a die attach process was developed to minimize the stresses on the DM induced by CTE mismatches between the DM (Silicon, 2.3ppm/K) and the ceramic package (Alumina, CTE, 7ppm/K).

Figure 9 shows the results of a study to compare the effects of the modulus of two different die attach adhesives used to bond the silicon MEMS DM die to the ceramic chip carrier. In this study, the surface figure of two 140 element DMs, mounted on Alumina chip carriers using epoxies with an elastic modulus of 1GPa and 3MPa was measured using an optical surface profiler while the ambient temperature was varied between -30C and 24C. Using the more compliant epoxy dramatically reduced the overall stress in the mirror facesheet of the MEMS DM such that the change in surface figure was within 100nm RMS compared to a variation of almost 1µm RMS with the stiffer epoxy. Additional studies will be performed to further decouple the DM from the ceramic package by increasing the bondline thickness.

7. 4096 CHANNEL DRIVE ELECTRONICS

To drive DM at frame rates of greater than 2.5 kHz drive electronics have been developed that provide 4096 parallel channels of drive voltages up to 285V with 14 bit resolution. This driver, shown in figure 10, uses a 200MB/s DIO interface and high density digital to analog converters in combination with high voltage amplifiers to achieve a 45µs latency (time between 1st word sent to last DAC written) corresponding to a frame rate of over 22kHz. Eight flexible cables carrying 512 signals each, carry the high voltage signals to the DM (see figure 10).

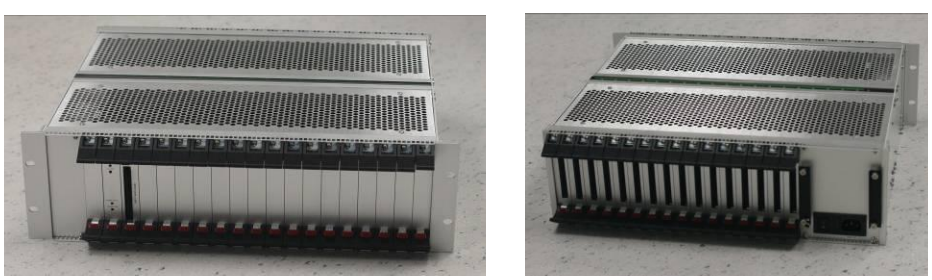

Figure 10. Compact 4096 element DM drive electronics (5.25"H x 19"W x 14"D): 200MB/s DIO input in front of chassis (left), 4096 high voltage outputs on rear of chassis (right).

8. DEVICE PERFOMANCE

The mechanical stroke (surface) of the DMs was measured by applying a known voltage to a 3x3 region of actuators and performing a differential measurement (subtracting 0V from test voltage measurement), using a white-light interferometer, to determine the device displacement. The results of three different DMs with different actuator design types are shown in figure 11.

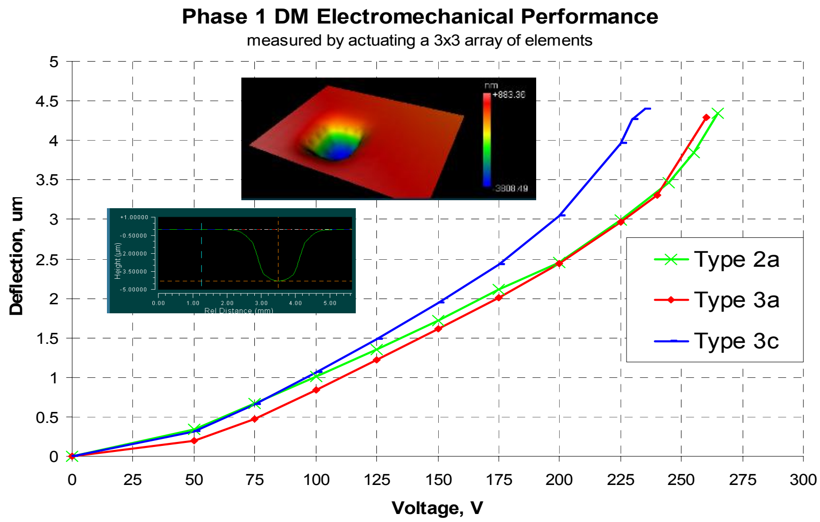

Figure 11. Voltage vs. displacement characteristics of various device types in which a 3x3 array is actuated to determine the maximum DM stroke. The small roll-off on some of the devices at maximum displacement is due to the mirror membrane touching down on actuator anchors.

These results indicate that all of the device types can achieve a surface stroke of over 3µm with sufficient margin over the critical deflection (indicated by the last data point on each curve). The operating voltage at 3.5µm stroke for all devices is between 210 and 260V.

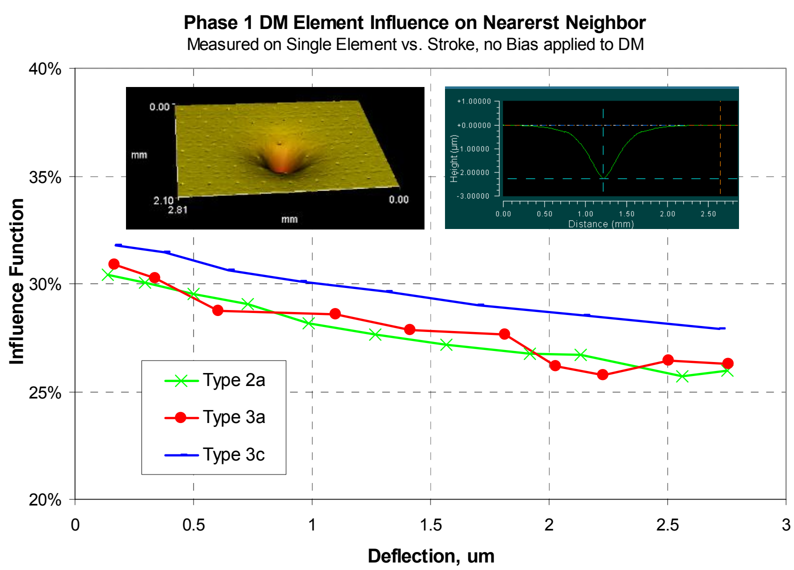

Figure 12. Influence function of the DMs as a function of DM element displacement. The influence function is tested with no bias applied to the other DM elements..

The device influence function was measured by actuating a single element and measuring the displacement of the neighboring actuator and comparing this to the displacement of the actuated element (see figure 12). The measured influence function was less than 32%, with a variation of less than 6%.

The inter-actuator stroke was measured by applying a sine-wave shape, with a period of 2 actuators, on a sub-array of DM elements as shown in figure 13. A voltage was applied to every other row in this sub-array to achieve this shape. Each of the three selected DM design types achieved an inter-actuator stroke larger than 1µm.

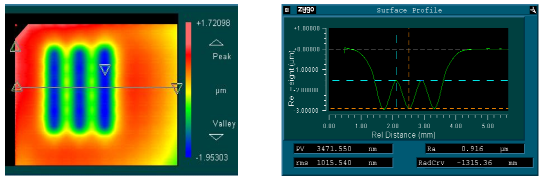

Device Type	Differential displacement, nm	Applied Voltage
Type 2a	1530	240
Type 3a	1770	230
Type 3c	1240	210

Figure 13. The inter-actuator stroke measured for the three DM design types is measured to be 1.2µm – 1.7µm.

The settling time of the DMs was measured by providing a step voltage input, corresponding to approximately 150nm displacement (typically 40-70V step) and measuring the DM's velocity response using a Polytec 3001 laser vibrometer and oscilloscope. The velocity response was integrated to obtain the device displacement responses which are summarized in figure 14. Each of the devices was measured to settle within 200µs.

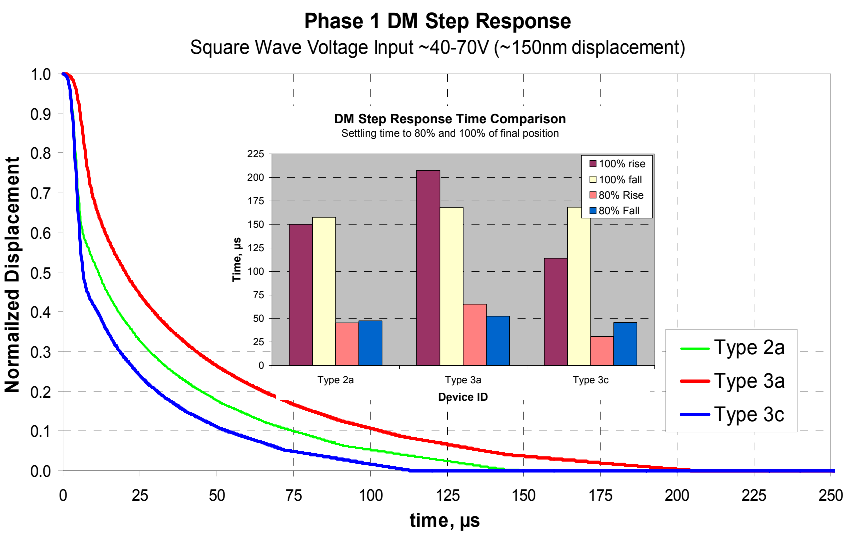

Figure 14. Normalized dynamic response of each of the three DM design types, to a square wave input of ~30V P-P, corresponding to a displacement of approximately 150nm. Each of the three devices settles within 200µs in response to the voltage step input.

9. CONCLUSION

The results from the first 4096 MEMS deformable mirror devices and its test devices show that the DM designs meets all the functional requirements for the high contrast imaging applications. Although the excessive bow of the DM surface is not correctable since the peak-to-valley is on the order of the total available stroke on the device, this surface figure error is low order and may be mitigated using corrective static optics to remove the curvature or a secondary "woofer" DM that would serve to remove the low order terms. The 4096 element MEMS DM is optimized for the compensation of high order aberrations at high frame rates that cannot be corrected for by other means.

10. ACKNOWLEDGEMENTS

This work has been support by the National Science Foundation Technology Center for Adaptive Optics managed by the University of California at Santa Cruz, and Lawrence Livermore National laboratories.

Thomas Bifano acknowledges a financial interest in Boston Micromachines Corporation.

REFERENCES

1. Macintosh, B., Graham, J., Oppenheimer, B., Poyneer, L., Sivaramakrishnan, A., Veran, J., "MEMS-Based Extreme Adaptive Optics for Planet Detection"**,** Proc. SPIE Vol. 6113, 611308 (Jan. 23, 2006)
2. Evans, J., Morzinski, K., Severson, S., Poyneer, L. Macintosh, B., Dillon, D., Reza, L., Gavel, D., Palmer, D., Olivier, S., and Bierden, P, "Extreme adaptive optics testbed: performance and characterization of a 1024-MEMS deformable mirror"**,** Proc. SPIE Vol. 6113, 61130I (Jan. 23, 2006)
3. Perreault, J. A., Bifano, T. G., Levine, B.M., and Horenstein, M., "Adaptive optic correction using microelectromechanical deformable mirrors," Opt. Eng. [41]5, pp. 561-566, 2002
4. Bifano, T., Perreault, J., Mali, R., et al., "Microelectromechanical deformable mirrors", IEEE J. of Selected Topics in Quantum Electronics, 5 (1): 83-89 Jan-Feb 1999.